

Luminescence properties of nanometer-sized Si crystallites: Core and surface states

Yoshihiko Kanemitsu

Institute of Physics, University of Tsukuba, Tsukuba, Ibaraki 305, Japan

(Received 28 January 1994)

We have studied the mechanism of visible photoluminescence (PL) from surface-oxidized Si crystallites of 3.7 nm diameter. Under intense laser-pulse illumination, two PL bands are clearly observed: a fast-decay blue-green PL band and a slow-decay red PL band. Time-resolved PL-spectrum measurements indicate that carriers generated in the core state are rapidly localized into the lower-energy surface states. Spectroscopic analysis indicates that the slow-decay red PL is caused by the hopping-limited recombination process in the surface-localized state of the crystallite, while the blue-green PL is caused by the band-edge emission from the core state of the crystallite.

There is currently intense interest in the optical and electronic properties of nanometer-sized semiconductor crystallites. The study of quantum size effects in nanometer crystallites made from direct-gap semiconductors such as CdSe,¹ CuCl,² etc. reveals that with a decrease in the crystallite size, the band-gap energy increases and the excited electronic states become discrete with high oscillator strength. Very recently, a great deal of research effort has been focused on indirect-gap semiconductor crystallites made from Si (Refs. 3 and 4) or Ge.⁵ However, despite many theoretical and experimental studies on the mechanism of the visible photoluminescence (PL) from porous Si and Si nanometer-sized crystallites, it still remains unclear.

With a large surface-to-volume ratio in nanometer-sized crystallites, the surface effects become more enhanced on decreasing the size of nanometer-sized crystallites. The presence of the crystallite surface as a boundary and source of surface states makes crystallites different from epitaxial low-dimensional structures,¹ and the surface effects as well as the quantum confinement effects control the optical and electronic properties of nanometer-sized crystallites.^{1,2} These two effects also complicate the mechanism of the broad visible PL in electrochemically etched porous Si.⁶ Time-resolved PL studies in porous Si (Refs. 7–10) indicate that the recombination processes are complex and the PL decay exhibits nonexponential behaviors. The broad PL spectrum and the nonexponential slow PL decay suggest that the disorder-induced localized state plays an important role in the radiative recombination process.^{7–10} We have little experimental understanding of the quantum confinement effects in porous Si. To clarify the mechanism of the visible PL in Si nanostructures such as porous Si, we need to fabricate Si nanocrystallite samples with an identical surface structure and to study the optical absorption and luminescence of isolated nanocrystallites.^{11,12}

In this paper, we report the photoluminescence properties of surface-oxidized Si crystallites with 3.7 nm diameter (the Si nanocrystallites capped by thin SiO₂ layer). There are two electronic states exhibiting a nonexponential slow-decay PL band at the red spectral region and a fast-decay PL band at the blue-green spectral region. Spectroscopic analysis leads us to propose a model in

which the red PL component originates from the surface localized state, while the blue-green PL component originates from the core state in the crystallite.

The nanometer-sized Si crystallites were produced by laser breakdown of SiH₄ gas. Pure SiH₄ gas was introduced into a vacuum chamber (a background pressure of $< 10^{-6}$ Torr) and the pressure of SiH₄ gas was held at 10 Torr. Laser pulses (~ 200 mJ per pulse at 1.06 μm , 10-ns pulse duration) from a Nd³⁺:YAG (yttrium aluminum garnet) laser system were focused. The Si crystallites deposited on quartz or Ge substrates were oxidized at room temperature in a chamber. Transmission electron microscopy, Fourier-transform infrared spectroscopy, and x-ray photoemission spectroscopy examinations¹¹ clearly indicate that the oxidized Si crystallites consist of a crystalline Si (*c*-Si) sphere of the 3.7-nm average diameter and an 1.6-nm-thick amorphous SiO₂ (*a*-SiO₂) surface layer.

Microsecond time-resolved PL spectra of oxidized Si crystallites were measured in a vacuum under 5-ns, 355-nm excitation (10-Hz repetition rate). The temperature was varied from 10 to 300 K in a cryostat. The spectral sensitivity of the measuring system was calibrated by using a tungsten standard lamp. In these experimental conditions, no significant fatigue of luminescence was observed.

Figure 1 summarizes the optical absorption, the PL spectrum under cw 325-nm laser excitation (weak laser illumination), and the first 200-ns time-averaged PL spectrum under 355-nm, 5-ns pulse excitation of (a) ~ 100 $\mu\text{J}/\text{cm}^2$ and (b) ~ 0.6 $\mu\text{J}/\text{cm}^2$ at room temperature. In the PL spectrum under cw laser excitation, a PL peak is around 760 nm and the PL spectrum is very broad [~ 0.3 eV full width at half maximum (FWHM)] with Gaussian-like shape. On the other hand, under pulse laser excitation, a PL band having a short lifetime is observed around 500 nm and this PL band becomes clear with increasing laser intensity. There is a weak absorption tail in the visible region and a strong absorption at the photon energy above 3 eV. It is pointed out that the blueshift of the optical absorption edge in Si nanocrystallites and the blue-green PL appears near the absorption edge.

Figure 2 shows the microsecond time-resolved PL from

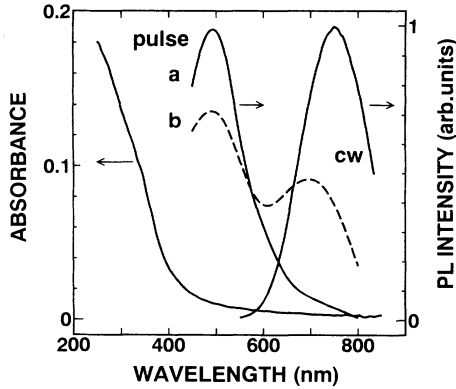


FIG. 1. Optical absorption spectrum, the photoluminescence spectrum under cw 325-nm laser excitation, and the first 200-ns averaged photoluminescence spectra under 5-ns, 335-nm pulsed laser excitation of (a) $\sim 100 \mu\text{J}/\text{cm}^2$ (solid line) and (b) $\sim 0.6 \mu\text{J}/\text{cm}^2$ (broken line) at room temperature.

oxidized Si crystallites. This figure was constructed from the spectrally resolved temporal response of photoluminescence. The decay of the red PL is slow, and the PL peak shifts to the longer wavelength with time delay. This suggests that carriers or excitons relax toward lower-energy states gradually. On the other hand, the decay of the blue-green PL band was very fast and the decay profile was not observed in the microsecond time region.

Figure 3(a) shows the red PL decay profiles at different wavelengths in the broad PL band at room temperature. The PL decay profiles are nonexponential, and they are well described by a stretched exponential function:¹³

$$I(t) = I_0(\tau/t)^{1-\beta} \exp[-(t/\tau)^\beta], \quad (1)$$

where τ is an effective decay time, β is a constant between 0 and 1, and I_0 is a constant. The solid lines in this figure are given by the above function. The least-squares fitting of the data gives values of τ and β . This stretched exponential decay is usually observed in the PL

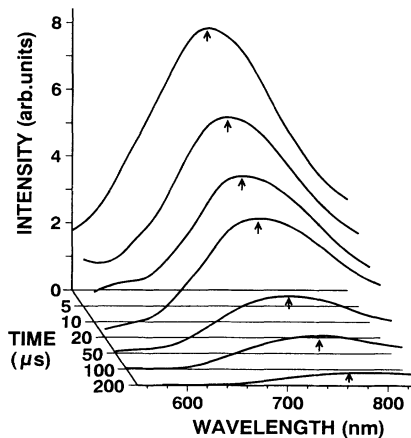


FIG. 2. Microsecond time-resolved photoluminescence spectra of oxidized Si nanocrystallites at room temperature under $\sim 70\text{-}\mu\text{J}/\text{cm}^2$ pulse laser excitation.

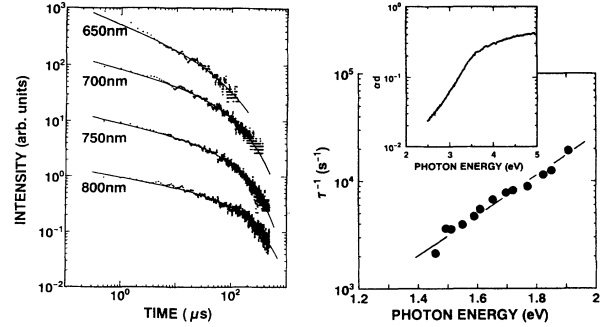


FIG. 3. (a) Double logarithmic plot of the decay curves at different wavelengths in the broad PL spectrum at room temperature. The solid lines are theoretical curves given by stretched exponential functions. (b) The PL decay rate τ^{-1} as a function of the photon energy. The inset is the absorbance αd vs the photon energy.

decay and transport properties of disordered system.¹³ The stretched exponential decay of the red PL suggests that the hopping motion of electrons and holes in localized states plays an important role in the PL process in Si nanocrystallites.

The decay time τ strongly depends on both the monitored PL photon energy and temperature. Figure 3(b) shows the dependence of the PL decay rate τ^{-1} on the PL photon energy E at room temperature. The exponential energy dependence of the decay rate is observed: The decay rate is approximately given by $\tau^{-1} \propto \exp(\Gamma_\tau E)$, where the straight line gives a value of $\Gamma_\tau \sim 3.4 \text{ eV}^{-1}$. Optical absorption measurements also indicate that the absorption edge has an exponential tail (the Urbach tail) in the visible spectral region, as shown in the inset of Fig. 3(b): The absorption tail is expressed as $\alpha d \propto \exp(\Gamma_\alpha E)$, where Γ_α is about 2.2 eV^{-1} and this value is slightly smaller than that of Γ_τ . We believe that the observed exponential energy dependence of the PL decay rate mainly reflects that of the density of localized states. Because the cascade of carriers from higher states to lower states makes the lifetime of higher states to be shorter, the exponential slope Γ_τ is larger than that of the density of states Γ_α . Moreover, the temperature dependence of τ^{-1} at a certain energy is given by $\tau^{-1} \propto \exp(-C/T^{1/3})$, where the factor C is a constant. This temperature dependence is also observed in electrochemically etched porous Si (Ref. 14) and is identical with the temperature dependence of the variable-range hopping of carriers in the two-dimensional systems. These characteristics of microsecond time-resolved PL (the stretched exponential PL decay, the exponential energy dependence of τ , and the temperature dependence of τ) strongly suggest that the disorder-induced carrier localization and the carrier hopping process in the quasi-two-dimensional surface region play a dominant role in the slow-decay red PL process in oxidized Si nanocrystallites.

Under intense pulse laser illumination, the transient blue-green PL band clearly appears near the absorption edge. Figure 4 shows the incident laser power dependence of the blue-green and red PL intensity. Even under intense laser illumination when the red PL inten-

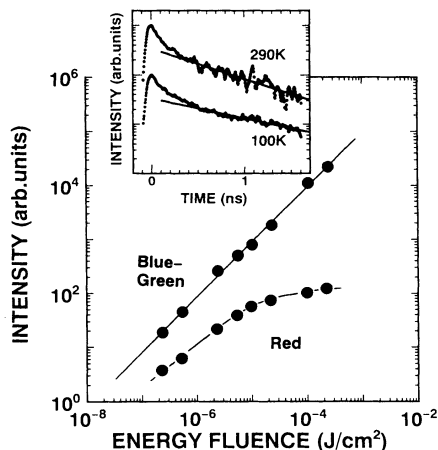


FIG. 4. Blue-green and red PL intensity at room temperature as a function of the incident nanosecond laser energy fluence per pulse. The inset is the picosecond PL decay at 500 nm. The solid lines are single exponential with time constants of ~ 1 ns at 100 K and ~ 0.8 ns at 290 K. The energy fluence dependence and decay dynamics of the blue-green PL are different from those of the red PL.

sity saturates, the blue-green PL intensity increases linearly with increasing laser intensity. Moreover, picosecond time-resolved PL spectra were measured by using a synchroscan streak camera and a 360-nm and 200-fs pulse from a cw-mode-locked Ti:Al₂O₃ laser (81-MHz repetition rate). The blue-green PL decay is very fast as shown in the inset of Fig. 4 (e.g., the solid lines are single exponential with time constants of about 1 ns at 100 K and about 0.8 ns at 290 K). There is no long component of the blue-green PL. Consequently, this PL band with a fast-decay rate and low efficiency (the time-integrated intensity ratio of the blue-green to the red PL is several percent or less) is not observed under cw laser excitation. These characteristics suggest that the mechanism of the blue-green PL is different from that of the red PL originating from the long-lived surface states and that the blue-green PL is the “band edge” emission from the core state of the crystallite.

Here we consider the origin of the red and blue-green PL in oxidized Si nanocrystallites. The band gap of the SiO₂ layer is out of the visible range (> 8 eV) and this layer does not itself contribute to the visible PL. However, it is theoretically pointed out that this SiO₂ layer creates an electronic state in an interface region between the *c*-Si core and SiO₂ layer.¹¹ The oxidized Si crystallite consists of two electronic states of the near-surface region and the *c*-Si core. Here, for simplicity, we consider the surface region as the one-sided oxidized planar Si sheet. The band gap of the fully oxygen-terminated Si sheet is calculated to be about 1.7 eV,¹⁵ which is roughly equal to the peak energy of the red PL. The band-gap energy of the 3.7-nm-diameter *c*-Si crystallite is about 2.4 eV,¹⁶ which is roughly equal to the peak energy of the blue-green PL. The band-gap energy of the oxygen-induced surface state is lower than that of the *c*-Si core. The surface roughness and the spatial fluctuation of the O

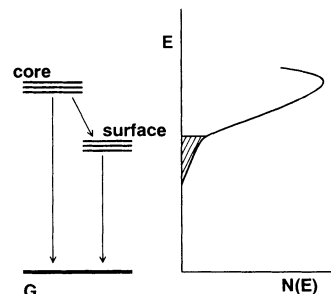


FIG. 5. Illustration of the density of states of oxidized Si nanocrystallites. The *c*-Si crystallite consists of two luminescent states: the *c*-Si core and the surface states. The band-gap energy of the 3.7-nm-diameter *c*-Si core is about 2.4 eV, while the band-gap energy of the oxidized surface region is about 1.7 eV. The density of localized states exponentially falls away from the *c*-Si core edge. The exponential tail (the Urbach tail) states are caused by the disordered surface states in the crystallites and the size distribution of the crystallites.

termination at the surface induce the energy distribution of the surface states. The band gap of one-sided oxidized Si sheet depends on the O-covering ratio: e.g., 2.0 eV in an incompletely oxidized (20% O-covering ratio) to 1.7 eV in fully oxidized (100% O terminated) Si sheet.¹⁵ These disordered surface effects cause the absorption tail and become more enhanced because of a large surface-to-volume ratio in nanometer-sized crystallites. In addition, the size distribution of the crystallites and defects in the *c*-Si core also contribute to the Urbach tail in the absorption spectrum. The density of states in our oxidized Si crystallite sample is illustrated in Fig. 5. The density of localized band-tail states exponentially falls off away from the *c*-Si core edge.

According to our energy diagram for oxidized Si crystallites, the radiative recombination process proceeds as follows: The photogeneration of carriers occurs within the core state, and a large number of the carriers are rapidly localized from the core state into the lower-energy localized surface states. The localized electrons and holes in the random potential (band tail) hop among localized states. If the hopping distance scarcely depends on the energy of the band-tail state, the lifetime of the red PL reflects the density of surface localized states. The difference between Γ_τ and Γ_α is caused by the hopping-down process (nonradiative process) from higher localized states into lower localized states. The redshift of the PL peak in the microsecond, the stretched exponential PL decay, and the exponential energy dependence of the PL decay rate is caused by the carrier-hopping-limited recombination process in surface localized states. On the other hand, under intense and short pulse illumination, the localized surface states show the population saturation, because the density of states is small and the recombination lifetime in localized states is microseconds or more. Then, some of the carriers remain in the core state and recombine radiatively in the core region. We observe the blue-green PL band-edge emission from the core state near the absorption edge. However, the blue-green PL decay is determined by the nonradiative process

in the core and the decay process from the core to the surface states, because the lifetime of the blue-green PL depends on temperature and the total intensity of the blue-green PL is lower than that of the red PL.

In as-prepared porous Si without air exposure, a very weak green PL is observed under cw laser excitation.¹⁷ After surface oxidation, a stable and strong PL band is observed at the red spectral region.^{10,17} The stretched exponential PL decay in these porous Si (Refs. 7–9 and 14) also suggests that the oxidized surface region becomes the localized states exhibiting strong and stable luminescence at the red spectral region. By removing the surface localized states exhibiting red PL, we expect to observe the “band-edge” luminescence from the core state even under cw laser excitation. For example, *ab initio* band-structure calculations¹⁵ suggest that the band-gap energy of the surface Si monolayer decreases with increasing the O-covering ratio (2.6 eV in the fully H-terminated Si sheet to 1.7 eV in the oxidized Si sheet). Because the band-gap energy of the H-terminated Si surface sheet is expected to be equal to or larger than that of the Si core with ~3 nm diameter, it is considered that the carefully controlled electrochemical method without air exposure

can reduce oxidized surface states exhibiting the red luminescence and cause blue-green luminescence from the core state in porous Si. In Si nanocrystallites, we can control the PL wavelength and the origin of the PL by changing either the excitation conditions (the laser pulse width and intensity in photoluminescence and the applied voltage in electroluminescence¹⁸) or the chemical structure of the crystallite surface.

In conclusion, we have studied time-resolved luminescence spectra to understand the nature of the core and surface states in 3.7-nm-diameter Si crystallites. Two PL components are observed: a fast component at the blue-green spectral region and a slow component at the red spectral region. The slow red component originates from the surface localized state of the crystallite and reflects the disorder nature of the Si nanocrystallite, while the fast blue-green component originates from the core region of the crystallite.

The author would like to thank H. Uto, Y. Yamada, Y. Masumoto, T. Ogawa, K. Takeda, and K. Shiraishi for helpful discussions. The author thanks the Sumitomo Foundation for financial support.

- ¹ M. G. Bawendi *et al.*, Phys. Rev. Lett. **65**, 1623 (1990); M. G. Bawendi, W. L. Wilson, P. J. Carroll, and L. E. Brus, J. Chem. Phys. **96**, 946 (1990).
- ² T. Itoh *et al.*, J. Lumin. (to be published).
- ³ L. T. Canham, Appl. Phys. Lett. **57**, 1046 (1990); A. G. Cullis and L. T. Canham, Nature **353**, 335 (1991).
- ⁴ V. Lehmann and U. Gosele, Appl. Phys. Lett. **58**, 856 (1991).
- ⁵ Y. Maeda *et al.*, Appl. Phys. Lett. **59**, 3168 (1991); Y. Kanemitsu *et al.*, *ibid.* **61**, 2178 (1992).
- ⁶ Y. Kanemitsu *et al.*, Phys. Rev. B **48**, 2827 (1993).
- ⁷ J. C. Vial *et al.*, Phys. Rev. B **45**, 14171 (1992).
- ⁸ N. Ookubo *et al.*, Appl. Phys. Lett. **61**, 640 (1992).
- ⁹ M. Kondo, J. Non-Cryst. Solids **164-166**, 941 (1993).
- ¹⁰ P. D. J. Calcott *et al.*, J. Phys. Condens. Matter **5**, L91 (1993).
- ¹¹ Y. Kanemitsu *et al.*, Phys. Rev. B **48**, 4883 (1993).

- ¹² K. A. Littau *et al.*, J. Phys. Chem. **97**, 1224 (1993).
- ¹³ K. L. Ngai, Comments Solid State Phys. **9**, 127 (1979); **9**, 141 (1980); K. L. Ngai and K. Murayama, Physica B+C **117/118**, 118 (1983).
- ¹⁴ Y. Kanemitsu, Phys. Rev. B **48**, 12357 (1993).
- ¹⁵ K. Takeda and K. Shiraishi, Solid State Commun. **85**, 301 (1993); K. Takeda, in *Light Emission from Novel Silicon Materials*, edited by Y. Kanemitsu, M. Kondo, and K. Takeda (The Physical Society of Japan, Tokyo, 1994), p. 1.
- ¹⁶ T. Takagahara and K. Takeda, Phys. Rev. B **46**, 15578 (1992).
- ¹⁷ See, for example, R. T. Collins *et al.*, Appl. Phys. Lett. **61**, 1649 (1992); V. M. Dubin *et al.*, J. Lumin. (to be published).
- ¹⁸ A. Biesy *et al.*, Phys. Rev. Lett. **71**, 637 (1993).